Extreme Mechanics Letters 22 (2018) 60–68

Contents lists available at ScienceDirect

Extreme Mechanics Letters

journal homepage: www.elsevier.com/locate/eml

Optimizing parameters to achieve giant deformation of an incompressible dielectric elastomeric plate

Yipin Su [a,b], Bin Wu [a,b], Weiqiu Chen [a,b,d,e], Chaofeng Lü [c,d,e,*]

[a] Department of Engineering Mechanics, Zhejiang University, Hangzhou 310027, PR China
[b] State Key Laboratory of Fluid Power and Mechatronic Systems, Zhejiang University, Hangzhou 310027, PR China
[c] Department of Civil Engineering, Zhejiang University, Hangzhou 310058, PR China
[d] Key Laboratory of Soft Machines and Smart Devices of Zhejiang Province, Zhejiang University, Hangzhou 310027, PR China
[e] Soft Matter Research Center, Zhejiang University, Hangzhou 310027, PR China

HIGHLIGHTS

- We investigate theoretically the nonlinear response and snap-through stability of a DE plate with strain-stiffening effect and electrostriction based on the so-called Hessian approach.
- We study the possibility of using snap-through instability and maximal allowable actuation strain to achieve large deformation of dielectric elastomeric plates.
- We construct three kinds of phase diagrams to reveal the underlying mechanism of how material properties and prestress influence the snap-through instability.
- We propose ways to design a type III DE by properly tuning the electrostriction, material stretchability and/or prestress.

ARTICLE INFO

Article history:
Received 19 January 2018
Received in revised form 23 May 2018
Accepted 23 May 2018
Available online 24 May 2018

Keywords:
Dielectric elastomer
Snap-through instability
Parameters optimization
Electroelasticity
Hessian approach

ABSTRACT

Snap-through instability can be readily utilized to acquire giant deformation of dielectric elastomeric structures. This study focuses on exploring such utilization by taking account of effects of intrinsic material properties, in addition to the extrinsic means (e.g. pre-deformation) that has been reported. Based on the recently proposed nonlinear formulations of electroelasticity and the so-called Hessian approach, we analyze theoretically the snap-through instability of an incompressible dielectric Gent elastomer plate sandwiched between two compliant electrodes subject to the combined action of electrical voltage and prestress. The snap-through instability occurs because of sudden decrease in the thickness and abrupt increase in the true electric field of the plate, and ceases at a state close to the limiting chain extensibility of the elastomer. By comparing the critical values for onset and stop of snap-through instability and electric breakdown of the elastomer, we study the possibility of using snap-through instability and maximal allowable actuation stretch to achieve large deformation. Three kinds of phase diagram are constructed to reveal the underlying mechanism of how material properties and prestress influence the snap-through instability. The results indicate that material properties and prestress may be tuned properly so as to achieve giant deformation of the plate.

1. Introduction

Traditional rigid devices expose a range of limitations such as cumbersome, inefficient and poorly adaptable. The last three decades have witnessed an explosion of applications of soft matters in actuators, soft robots, bioengineering and medical devices. With the advantages of high-sensitivity, low noise and high efficiency, flexible structures or soft machines made of soft matter are becoming the core technology for the next-generation functional devices [1–4]. Dielectric elastomers (DEs) are a kind of soft electroactive materials. They can undergo large voltage-induced strains with fast response that cannot be achieved in other soft materials such as rubbers and biological tissues, and therefore, are perfectly suitable for sensors and actuators [5–9]. A typical highly deformable dielectric actuator consists of a soft elastomeric material sandwiched between two compliant electrodes, through

* Corresponding author at: Department of Civil Engineering, Zhejiang University, Hangzhou 310058, PR China.
E-mail address: lucf@zju.edu.cn (C. Lü).

https://doi.org/10.1016/j.eml.2018.05.004
2352-4316/

which an applied voltage may generate attractive forces so as to cause reduction in thickness and expansion in area of the actuator.

Generally, to obtain giant voltage-induced strains, DEs often work in extremely high voltage conditions, thus making DEs susceptible to various failure modes such as Euler buckling, loss of tension and electrical breakdown [10–18]. These features have long been recognized in the electrical power industry as failure modes of polymer insulators and pose clear limitations on developing DE devices. Of special interest is the snap-through or electromechanical instability, accompanied by the coexisting state of both flat and wrinkled regions in the dielectric film when the applied voltage reaches a threshold [19]. Increasing research effort has been devoted to harnessing the snap-through instability of DEs [20–29], and giant areal strains (say, more than 1000%) have been reported experimentally [30–32].

Zhao and Suo [20] proposed the so-called Hessian method to reveal the underlying physical mechanism of electromechanical instability of a DE plate. When subjected to a voltage across its thickness, a DE plate contracts in the thickness direction and expands along the in-plane directions. The thickness contraction leads to an increase in the electric field, which may drive the elastomer to thin down drastically. They showed that the electromechanical instability occurs when the Hessian matrix, also termed as the generalized tangent modulus, ceases to be positive definite. During the thinning procedure, the true electric field of the DE plate increases, thus inducing an electrical breakdown. The authors applied this method to analyze the electromechanical instability of an incompressible plate modeled as ideal neo-Hookean dielectric solid and successfully predicted the onset of instability, which agrees very well with existing experimental observations. Nevertheless, the snap-through behavior was not presented in their prediction because the so-called strain-stiffening effect, an essential attribute of most realistic materials, is absent in the considered material model. By comparing the critical values for the onset and stop of snap-through instability with that for electrical breakdown, Koh et al. [33] generalized three types of DE materials and analyzed the corresponding nonlinear responses (Fig. 1). Obviously, dielectric elastomer of type III is the most ideal material since its allowable maximal actuation strain is much larger than those of types I and II. So far, little attention has been devoted to the control of snap-through behavior excited by the onset of electromechanical instability, and the design of a type III dielectric to achieve giant deformation still remains an unrevealed topic.

In this paper, the nonlinear response of a DE plate subjected to the combined action of voltage and prestress is investigated and the so-called Hessian method formulated by Zhao and Suo [20] is adopted to investigate the snap-through instability of the plate. Three different kinds of phase diagram are for the first time, constructed (Figs. 4, 8 and 13) for our particular purpose of gaining giant deformation by properly selecting the system parameters, including prestress, material stretchability and dielectricity. Based on these phase diagrams, we propose three methods to design a type III dielectric by tuning material parameters and prestress. The results demonstrate that material constants and prestress significantly influence the non-linear response and snap-through instability of the plate, and an optimal type of DE material with maximal allowable actuation stretch can be designed by properly tuning the material constants.

2. Governing equations

Consider an incompressible, isotropic DE plate with initial dimensions L_1, L_2 and H depicted in Fig. 2. The plate is coated on the top and bottom faces with flexible electrodes (typically, by brushing on carbon grease). Subjected to a combined action of equi-biaxial nominal tensile stress P in the plate plane and voltage V between the electrodes, the DE plate deforms homogeneously from the undeformed configuration to the deformed configuration, which is generally accompanied by the expansion in the area and deduction in the thickness of the plate. The finite isochoric deformation can be described by the mapping

$$x_1 = \lambda X_1, x_2 = \lambda X_2, x_3 = \lambda^{-2} X_3, \tag{1}$$

where X_1, X_2, X_3 and x_1, x_2, x_3 correspond respectively to Cartesian coordinate systems of undeformed and deformed configurations, while λ is the principal stretch of lateral dimensions. Then, the deformation gradient tensor is given by $\mathbf{F} = \mathrm{diag}\left(\lambda, \lambda, \lambda^{-2}\right)$. Since the thickness of the plate is small compared with the lateral dimensions L_1 and L_2, the fringe effect can be ignored and the true (nominal) electric field is taken to be homogeneous across the plate thickness $E = V/h$ ($E_0 = V/H$), where $h = \lambda^{-2} H$ is the thickness of the deformed plate.

At this stage we note that the energy function has only two independent variables. As an illustrative example, we consider the following free-energy function

$$W(\lambda, D_0) = -\frac{\mu G}{2} \ln\left(1 - \frac{2\lambda^2 + \lambda^{-4} - 3}{G}\right) + \frac{1}{2\varepsilon}\frac{D_0^2}{\lambda^4}. \tag{2}$$

where μ is the shear modulus of the material, $G = 2\lambda_{\mathrm{lim}}^2 + \lambda_{\mathrm{lim}}^{-4} - 3$ is called the Gent constant that is related to the limiting chain extensibility of incompressible rubber networks, D_0 is the nominal electric displacement, and ε denotes the electric permittivity of the elastomer. In Eq. (2), the first term is the Gent energy function [34] due to elastic deformation, which recovers the neo-Hookean model that describes a solid with unlimited stretchability for $G \to \infty$. The second term of the energy function stands for the contribution of the polarization effect. Here we adopt a linear deformation-dependent permittivity [35] which is proposed by calibrating the experimental measurements [36], i.e.

$$\varepsilon = k\varepsilon_0 \left[1 + 2c(\lambda - 1)\right], \tag{3}$$

where $\varepsilon_0 = 8.85$ pF/m is the permittivity of vacuum, the constant $k = 4.68$ is fitted from experimental data of VHB 4910 (an acrylic elastomer produced by 3M) [36], and c is the coefficient of electrostriction. For the case $c = 0$, the dielectric permittivity is deformation-independent and the energy function in Eq. (2) reduces to the so-called ideal dielectric model [20].

Using the framework of nonlinear electroelasticity [37,38], the constitutive equations of a biaxially stretched dielectric are obtained as [39]

$$P = \frac{1}{2}\frac{\partial W}{\partial \lambda}, E_0 = \frac{\partial W}{\partial D_0}. \tag{4}$$

It should be noted that the in-plane boundary condition $T_{11} = T_{22} = P$ has been used, where T_{ij} is component of the nominal stress tensor. Combining with the energy function (2) and the permittivity (3), we get the constitutive relations as

$$\overline{P} = \frac{\overline{D}_0^2\left[c(4 - 5\lambda) - 2\right]}{2\lambda^5[1 + 2c(\lambda - 1)]^2} - \frac{G(\lambda^6 - 1)}{\lambda + 2\lambda^7 - \lambda^5(G + 3)}, \tag{5}$$

$$\overline{E}_0 = \frac{\overline{D}_0}{\lambda^4\left[1 + 2c(\lambda - 1)\right]}, \tag{6}$$

where the following dimensionless quantities have been employed

$$\overline{P} = \frac{P}{\mu}, \overline{E}_0 = E_0\sqrt{\frac{k\varepsilon_0}{\mu}} = \frac{V}{H}\sqrt{\frac{k\varepsilon_0}{\mu}}, \overline{D}_0 = \frac{D_0}{\sqrt{k\mu\varepsilon_0}}. \tag{7}$$

Eqs. (5) and (6) establish the correlations between the non-dimensional nominal electric field $\overline{E}_0$, the non-dimensional nominal electric displacement $\overline{D}_0$ and the stretch λ for a given applied

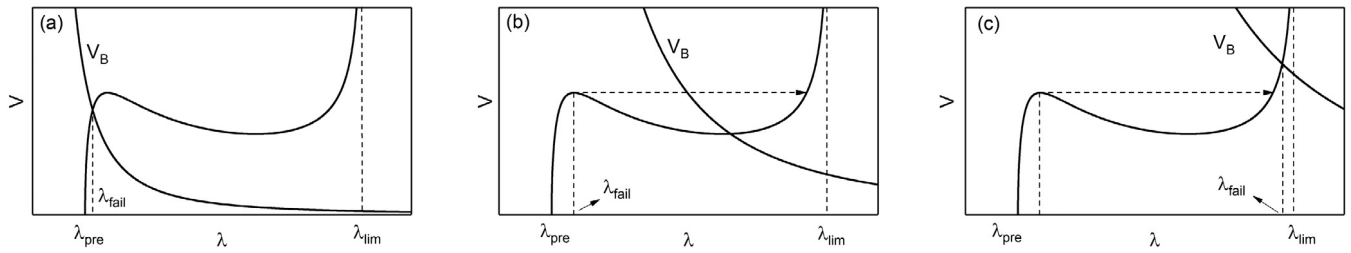

Fig. 1. Three types of DEs [33]: (a) Electrical breakdown prior to the onset of snap-through instability (type I); (b) Electrical breakdown happens during the snap-through instability process (type II); (c) The DE material survives the snap-through instability (type III).

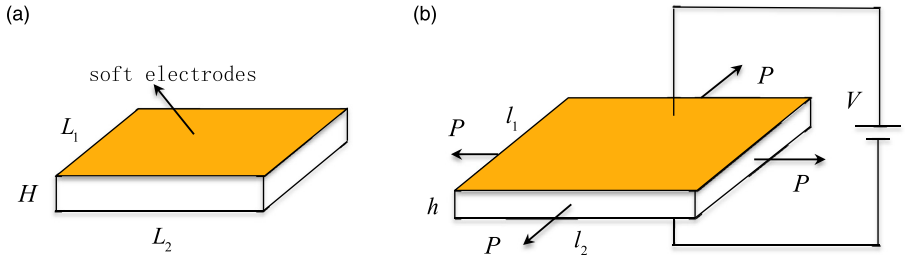

Fig. 2. A DE plate subjected to equi-biaxial stretch with a voltage normal to the major surfaces: (a) Undeformed configuration; (b) Deformed configuration.

non-dimensional mechanical load $\overline{P}$. The two equations govern the nonlinear behavior of the DE plate. Throughout this paper, we focus on the so-called actuation stretch λ/λ_0 of the plate, which is more meaningful than the stretch λ from industrial aspect. Here, we designate λ_0 (i.e. λ_{pre} in Fig. 1) as the prestretch due to the mechanical loads in the absence of applied voltage, which can be determined through the equation

$$\overline{P} = -\frac{G(\lambda^6 - 1)}{\lambda + 2\lambda^7 - \lambda^5(G+3)}. \tag{8}$$

Thermodynamic analysis shows that the snap-through instability of the DE plate will occur when the determinant of the following matrix, called the Hessian or generalized tangent modulus, is zero,

$$\mathbf{H}_e = \begin{bmatrix} \dfrac{\partial^2 W}{\partial \lambda^2} & \dfrac{\partial^2 W}{\partial \lambda \partial D_0} \\ \dfrac{\partial^2 W}{\partial \lambda \partial D_0} & \dfrac{\partial^2 W}{\partial D_0^2} \end{bmatrix}, \tag{9}$$

which leads to

$$\frac{G\lambda^4[1+2c(\lambda-1)]^3\left[5\lambda^4(G+3)+\lambda^{10}(G+3)+2\lambda^{12}-19\lambda^6-1\right]}{\left[2\lambda^7-\lambda^4(G+3)+1\right]^2} - D_0^2[1+2c(\lambda-1)][3+2c(5\lambda-3)] = 0, \tag{10}$$

with the help of Eqs. (2) and (3).

3. Numerical results and discussions

Based on the above analysis, the nonlinear behavior and snap-through instability of an ideal DE plate ($c = 0$) without applied prestress ($\overline{P} = 0$) is first studied for illustration. The dependences of the nominal (true) electric field $\overline{E}_0$ ($\overline{E}$) and the determinant of the Hessian matrix det($\mathbf{H}_e$) on the nominal electric displacement $\log_{10}\overline{D}_0$ are presented in Fig. 3(a) and (b), while the dependences of the nominal electric displacement (field) $\log_{10}\overline{D}_0$ ($\overline{E}_0$) and the determinant of the Hessian matrix det($\mathbf{H}_e$) on the principal stretch λ are depicted in Fig. 3(c) and (d). It can be seen that as the applied voltage increases within a range of small magnitude, the stretch λ and all electrical relative quantities $\overline{E}_0$, $\overline{E}$, $\overline{D}_0$ increase while det($\mathbf{H}_e$) decreases monotonically. At this stage the plate remains stable since det($\mathbf{H}_e$) > 0 is always satisfied until the voltage reaches a peak value (stage A) at which det($\mathbf{H}_e$) $= 0$. An ascending perturbation in the applied voltage may drive the plate to the so-called snap-through instability, jumping from stage A to stage C rather than varying along the dotted $A-B-C$ curve. As the applied voltage further increases, the plate becomes stable again since det($\mathbf{H}_e$) > 0 holds again. During this process, the nominal electric field $\overline{E}_0$ is always continuous but there will be a sudden jump in $\overline{E}$, $\overline{D}_0$ and λ.

In these calculations, we take $G = 97.2$, which indicates that the limiting stretch of the material is $\lambda_{\lim} = 7.08$ in elongation. This limiting stretch was measured by Gent [34] for vulcanized rubber and was recently used by Dorfmann and Ogden [40,41] to simulate the nonlinear responses of dielectric materials. When the applied voltage is small, the slopes of curves in Fig. 3(c) and (d) are large, implying that the plate thins down slowly as the voltage increases till λ reaches a threshold value, surpassing which the snap-through instability happens with a drastic increase in λ. Consequently, the polymer chains approach an extension limit $\lambda_{\lim} \approx 7.08$ and the snap-through stops. That is, the plate will experience a post-stable state after the snap-through instability happens. This should attribute to the strain-stiffening effect induced by the finite stretchability of the material, which is absent in the neo-Hookean material [20].

To further investigate the dependence of snap-through instability of the plate on material parameters (G, c) and prestress ($\overline{P}$) and to compare directly the snap-through instability with the electrical breakdown, we extract $\overline{E}_A$ and $\overline{E}_C$ corresponding to the critical values of onset and stop of snap-through instability in the $\overline{E} \sim \log_{10}\overline{D}_0$ plots for a continuous spectrum of $G, \overline{P}, c$, and plot respectively the $\log_{10}\overline{E} \sim \log_{10}G$, $\log_{10}\overline{E} \sim \overline{P}$ and $\log_{10}\overline{E} \sim c$ relations in Figs. 4, 8 and 13, which represent the phase diagrams regarding the stability of a DE plate.

Fig. 4 exhibits the dependences of $\overline{E}_A$ and $\overline{E}_C$ of the plate with $\overline{P} = 0, c = 0$ on the stretchability G. The $\log_{10}\overline{E}_A \sim \log_{10}G$ curve is nearly horizontal and, together with the curves in Fig. 5, we can conclude that the response of the DE plate to the electric stimulus is independent of G before the snap-through instability is triggered, while $\log_{10}\overline{E}_C$ is nearly linearly dependent on $\log_{10}G(\leq 2.35$, i.e., $G \leq 225)$. The $\log_{10}\overline{E} - \log_{10}G$ plane is divided into two regions corresponding to stable and snap-through domains by the

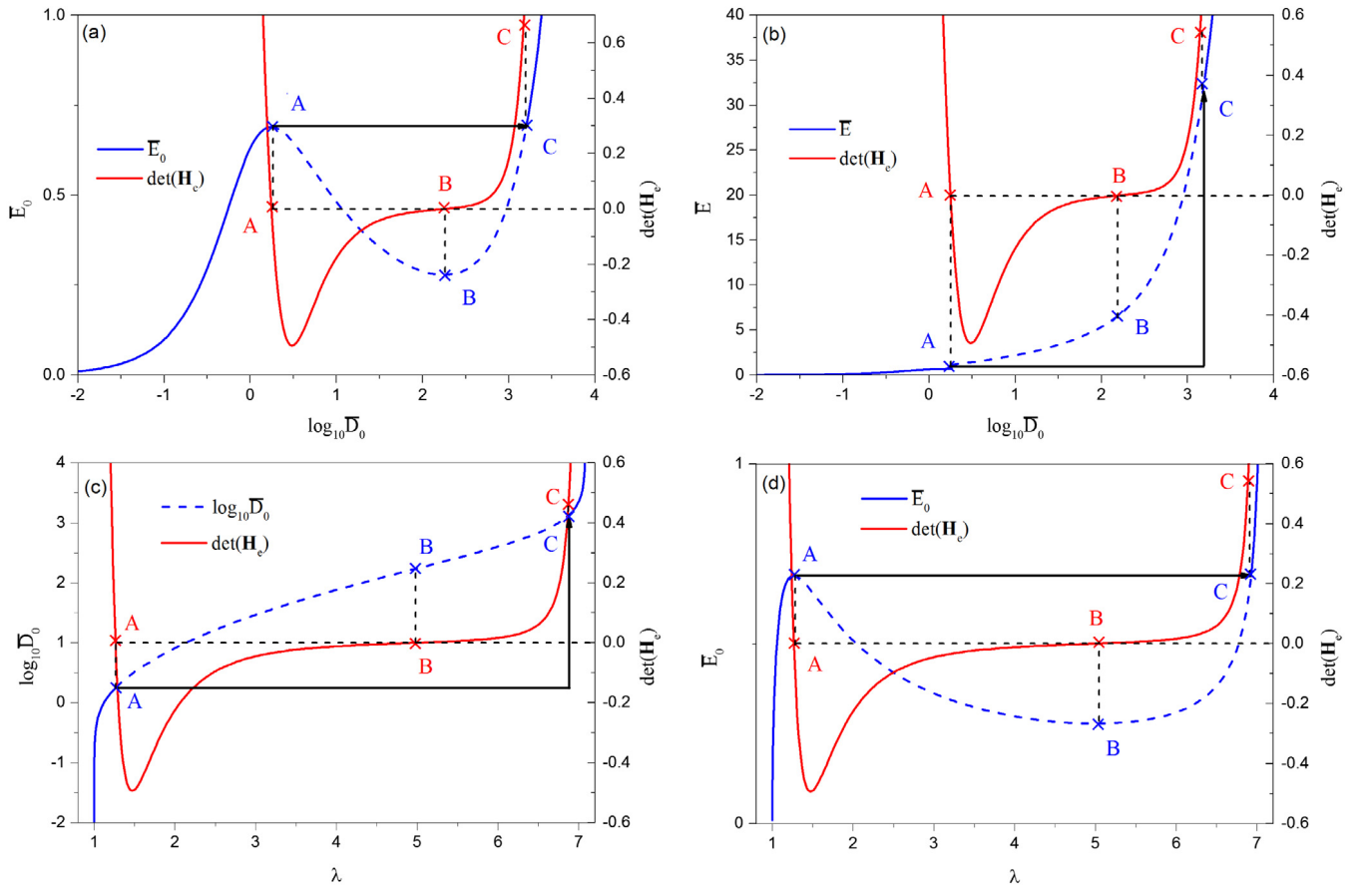

Fig. 3. Nonlinear response of a DE plate with $G = 97.2$, $\bar{P} = 0$, $c = 0$: (a) Plots of $\bar{E}_0$ and $\det(\mathbf{H}_e)$ versus $\log_{10}\bar{D}_0$; (b) Plots of $\bar{E}$ and $\det(\mathbf{H}_e)$ versus $\log_{10}\bar{D}_0$; (c) Plots of $\log_{10}\bar{D}_0$ and $\det(\mathbf{H}_e)$ versus λ; (d) Plots of $\bar{E}_0$ and $\det(\mathbf{H}_e)$ versus λ.

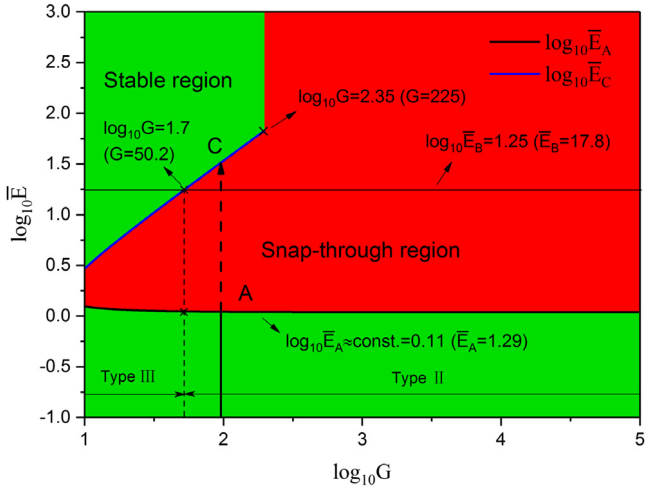

Fig. 4. Phase diagram of stable and unstable domains of a DE plate with $\bar{P} = 0$, $c = 0$, with which the snap-through procedure of a DE with given material property G can be specified. The type of the material can be determined with the prescribed non-dimensional breakdown voltage $\bar{E}_B = 17.8$.

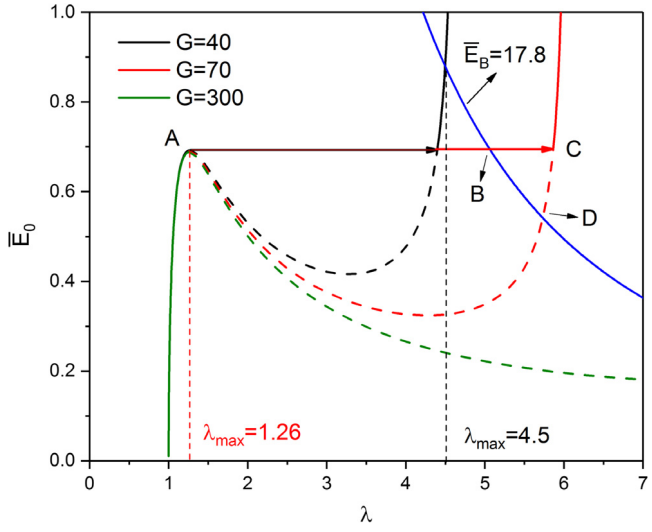

Fig. 5. Plots of $\bar{E}_0 \sim \lambda$ for a range of $G = 40, 70, 300$ for a DE plate with $\bar{P} = 0, c = 0$. We can see that material with $G = 40$ belongs to type III while material with $G = 70$ or 300 belongs to type II, and material with $G = 300$ behaves like a neo-Hookean material.

$\log_{10}\bar{E}_A \sim \log_{10}G$ and $\log_{10}\bar{E}_C \sim \log_{10}G$ curves. It can be seen that after reaching a threshold true electric field $\bar{E}_A(\approx 1.29)$ which is independent of G, the plate experiences a snap-through process with dramatical decrease in thickness and eventually achieves a larger true electric field $\bar{E}_C$, which depends on G. Note that the snap-through instability stops at a state close to the limiting stretch for $G \leq 225$ due to the stiffening effect which is absent in the neo-Hookean like material with $G > 225$. Once the snap-through occurs, the thickness of plate with $G > 225$ will decrease sequentially, leading to electrical breakdown.

It is well known that a DE plate may fail upon electrical breakdown when subjected to a sufficiently large voltage. Pelrine et al. [42] have measured and listed the dielectric strength of sev-

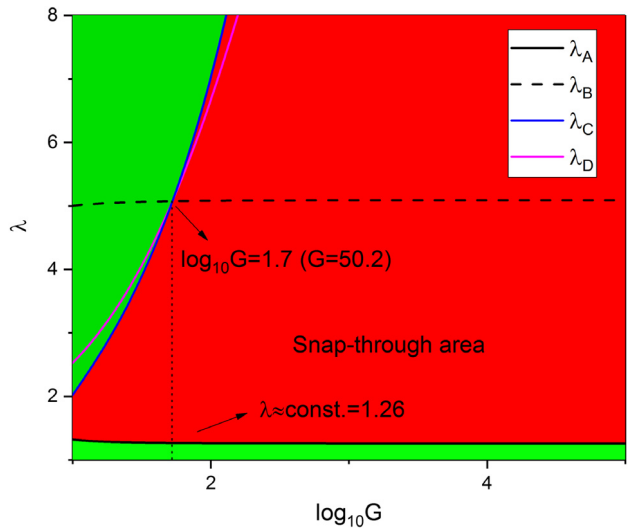

Fig. 6. Phase diagram of critical stretches of a DE plate with $\overline{P} = 0, c = 0$. Based on this diagram, the allowable maximal stretch of the DE plate with given material property G can be determined.

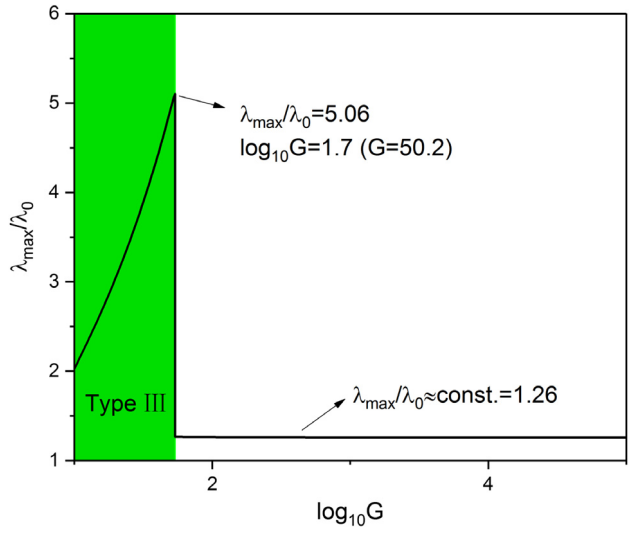

Fig. 7. Plot of λ_{max}/λ_0 versus $\log_{10}G$ of a DE plate with $\overline{P} = 0, c = 0$. The maximal actuation stretch of a DE plate with $\log_{10}G > 1.7$ (or $G > 50.2$) is constrained by electrical breakdown, which will occur first before the plate stops to be stable again once the snap-through instability is activated.

eral specific dielectric materials (see Table 1 therein). Here, in our calculations, the non-dimensional true breakdown electric field $\overline{E}_B$ of a DE plate is assumed to be constant and independent of G, c, $\overline{P}$ and is taken to be 17.8 according to the credible experimental measurements [33,42]. Then the corresponding non-dimensional nominal breakdown electric field can be obtained as $\overline{E}_{0B} = \overline{E}_B/\lambda^2$. It is seen from Fig. 4 that for $G \leq 50.2$, the plate behaves as a type III DE, i.e., it survives the snap-through instability and a larger maximal stretch can be attained for material with larger G. While plate with $G > 50.2$ will fail because of electrical breakdown during the snap-through procedure. Thus the optimal material constant is $G = 50.2$, with which the plate may acquire the largest maximal stretch $\lambda_{max} \approx 5$, utilizing the snap-through instability. The allowable maximal stretch of type III DE is considerably larger than that of type II DE (Fig. 5). With the help of the $\log_{10}\overline{E} \sim \log_{10}G$ phase diagram (Fig. 4), a reasonable polymeric extensibility G may be chosen to acquire a type III DE.

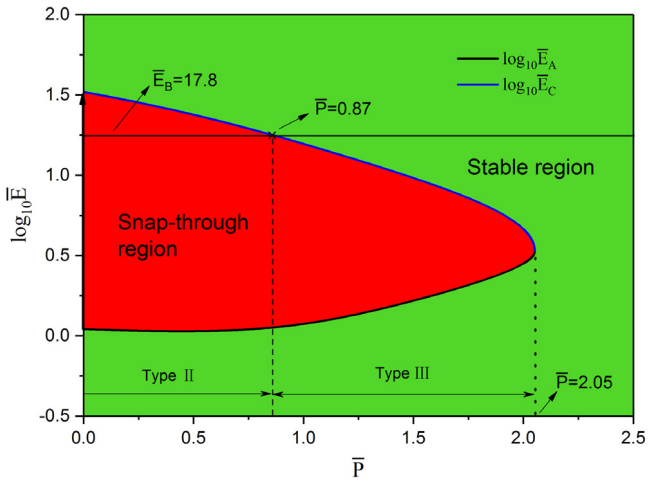

Fig. 8. Phase diagram of stable and unstable domains of a DE plate with $G = 97.2, c = 0$. A large enough prestress may suppress the snap-through instability of the plate.

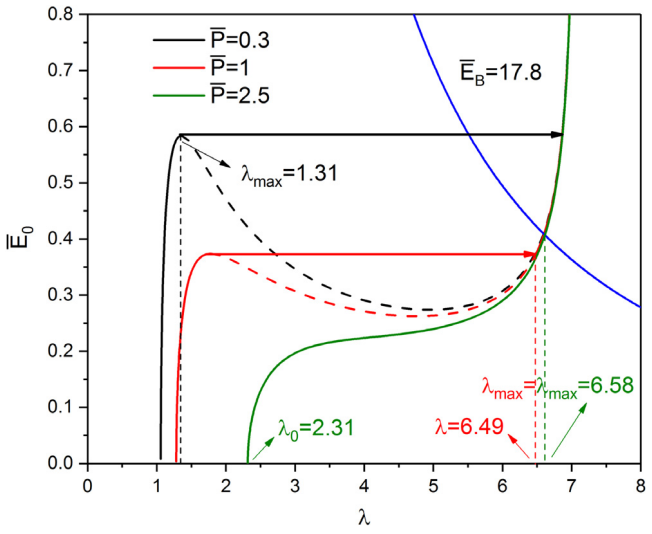

Fig. 9. Plots of $\overline{E}_0 \sim \lambda$ for $\overline{P} = 0.3, 1, 2.5$ for a DE plate with $G = 97.2, c = 0$. We can see that prestress can significantly influence the critical values of both the onset and stop of snap-through instability.

To specify the allowable deformation of a DE plate, we then further investigate some critical stretches of the plate. Here we designate λ_A and λ_C as the critical stretches of the onset and stop of snap-through instability, respectively, λ_B as the stretch of the point on $\overline{E}_B = 17.8$ curve that has the same nominal electric field as points A and C, while λ_D as the stretch of the cross point of $\overline{E}_0 \sim \lambda$ and $\overline{E}_B = 17.8$ curves (see the curve of $G = 70$ in Fig. 5). We extract λ_A, λ_B, λ_C and λ_D in the $\overline{E}_0 \sim \lambda$ plots for a continuous spectrum of G to generate the phase diagram of critical stretch of a DE plate (Fig. 6). For plates with $G < 50.2$, after snap-through deformation from λ_A to λ_C, the plate can be further stretched by increasing the applied voltage until it fails at λ_D because of electrical breakdown. In contrast, plates with $G \geq 50.2$ cannot be further stretched after reaching λ_A, beyond which the plate will experience electrical breakdown at λ_B during the snap-through deformation. Utilizing this phase diagram (Fig. 6), we can obtain the maximal allowable actuation stretch λ_{max}/λ_0 (Fig. 7, where $\lambda_0 = 1$) of the plate with a specified G, here λ_{max} is the allowable maximal stretch of the plate. It can be seen from Fig. 7 that λ_{max}/λ_0 increases with G (<50.2) and the plate with $G = 50.2$ performs the best.

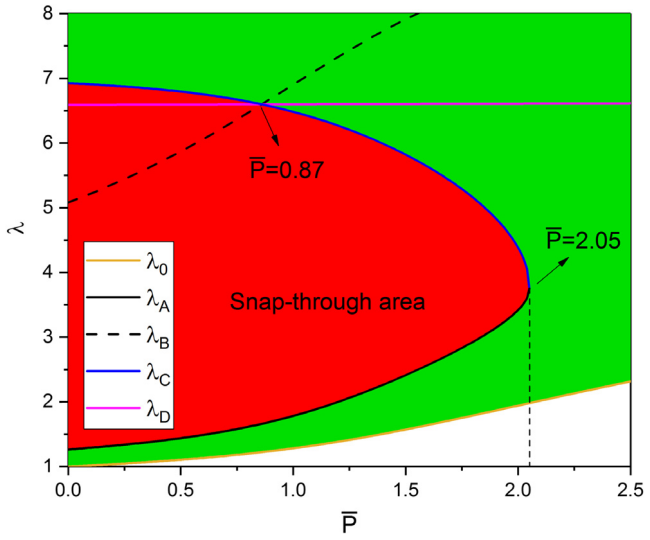

Fig. 10. Phase diagram of critical stretches of a DE plate with $G = 97.2$, $c = 0$. The optimal prestress is $\overline{P} = 0.87$, larger than which the plate survives the snap-through instability while the actuation stretch of the plate decreases as $\overline{P}$ increases.

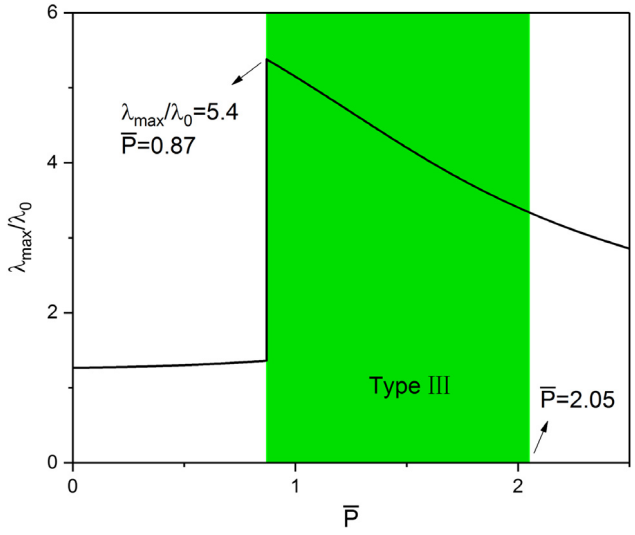

Fig. 11. Plot of λ_{max}/λ_0 versus $\overline{P}$ of a DE plate with $G = 97.2$, $c = 0$. To maximize the actuation stretch, a prestress of $\overline{P} = 0.87$ is needed.

Fig. 8 displays the dependence of the snap-through instability of the plate with $G = 97.2$, $c = 0$ on the prestress $\overline{P}$. The critical value of the true electric field $\overline{E}_A$ to activate the snap-through instability increases and the snap-through stops with a decreasing $\overline{E}_C$ as the prestress increases, indicating that the prestress poses a significant stabilizing effect on the snap-through instability of the DE plate. Moreover, the snap-through instability of the plate may be suppressed once the applied prestress reaches a sufficiently large value (e.g. $\overline{P} > 2.05$). After the application of voltage, the prestressed DE plate deforms starting from λ_0 (Fig. 10). For plate with $\overline{P} \leq 0.87$, snap-through deformation occurs at λ_A, and the plate fails due to electrical breakdown at λ_B, rather than stops at λ_C. As the prestress increases and exceeds 0.87, the plate will survive the snap-through instability and can be further deformed until electrical breakdown at λ_D. The optimal prestress is $\overline{P} = 0.87$ (Fig. 11). At this stage the resulting stretch activated by snap-through instability is giant while the driving voltage needed for the awake of snap-through instability of the plate is relatively low. As the applied force further increases, the applied voltage needed to drive the snap-through increases while the snap-through induced deformation decreases. For the plate subjected to $\overline{P} > 2.05$, the snap-through is suppressed and the plate always fails at a larger stretch $\lambda_{max} = 6.58$ due to the electrical breakdown (Fig. 9). However, the maximal actuation stretch λ_{max}/λ_0 is relatively small (e.g., for $\overline{P} = 2.5$, $\lambda_{max}/\lambda_0 \approx 2.85$, while for $\overline{P} = 0.87$, $\lambda_{max}/\lambda_0 = 5.4$).

We further investigate the influences of the coefficient of electrostriction c and material stretchability G on the $\log_{10}\overline{E} \sim \overline{P}$ phase diagram of a DE plate (Fig. 12). Decreasing c or G will increase $\overline{E}_A$ and simultaneously decrease $\overline{E}_C$. As a result, the DE plate may always survive snap-through instability, independent of $\overline{P}$ (see the areas enclosed by the dotted curves in Fig. 12, which always beneath the non-dimensional true breakdown electric field $\overline{E}_B = 17.8$).

Zhao and Suo [35] studied the nonlinear responses of dielectric materials with various values of the coefficient of electrostriction c ($c = -0.053$ corresponds particularly to the acrylic elastomer VHB 4910 [36]). They pointed out that the Maxwell stress can be partially removed by the effect of the deformation-dependent permittivity for the case $c < 0$, and moreover the snap-through instability will be suppressed if c is sufficiently small. Their model (e.g. $c = -10$) can predict specific dielectrics which become thicker under an applied voltage. The effects of the coefficient of electrostriction c (which is selected to be within the reasonable range predicted by Zhao and Suo [35]) on the snap-through instability and allowable stretch of a DE plate with $G = 97.2$, $\overline{P} = 0$

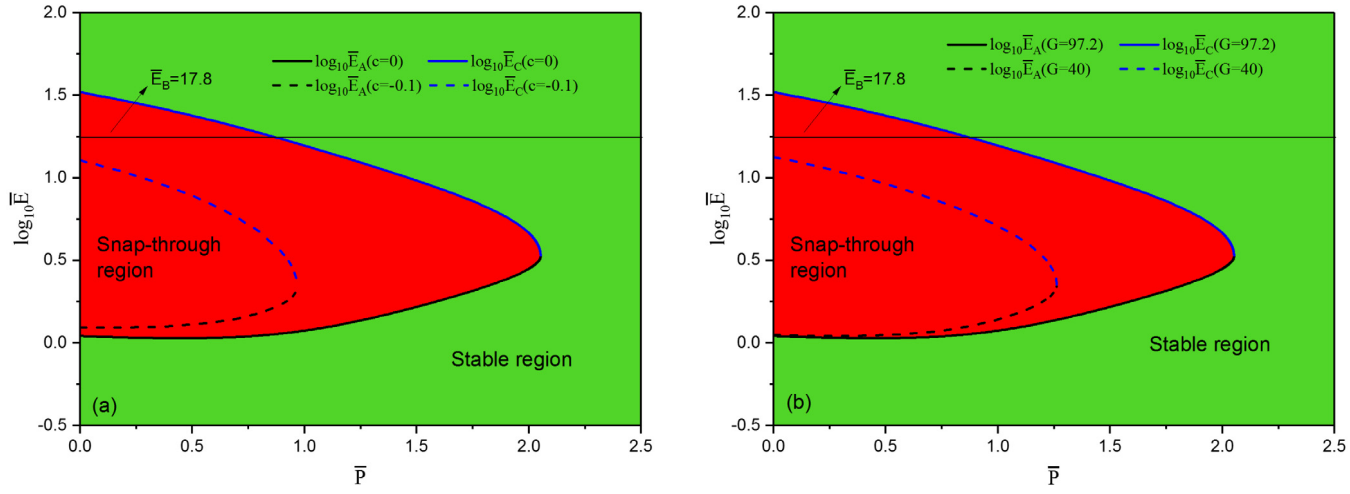

Fig. 12. Phase diagram $\log_{10}\overline{E} \sim \overline{P}$ of a DE plate with (a) constant $G = 97.2$ and various c; (b) constant $c = 0$ and various G.

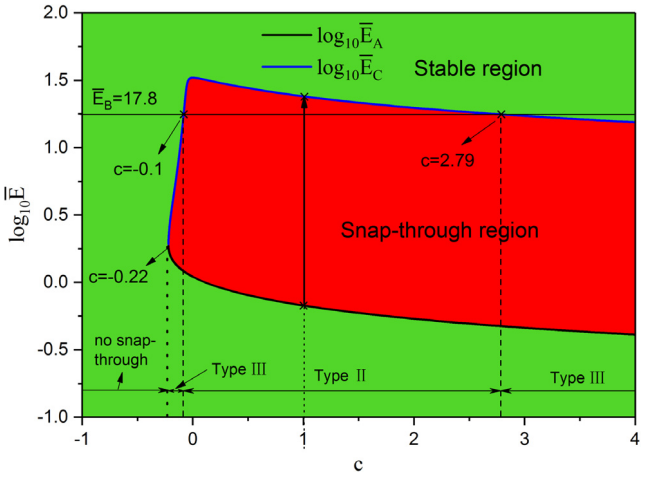

Fig. 13. Phase diagram of stable and unstable domains of a DE plate with $G = 97.2$, $\overline{P} = 0$. The snap-through instability of a plate with sufficiently small electrostriction c may be suppressed.

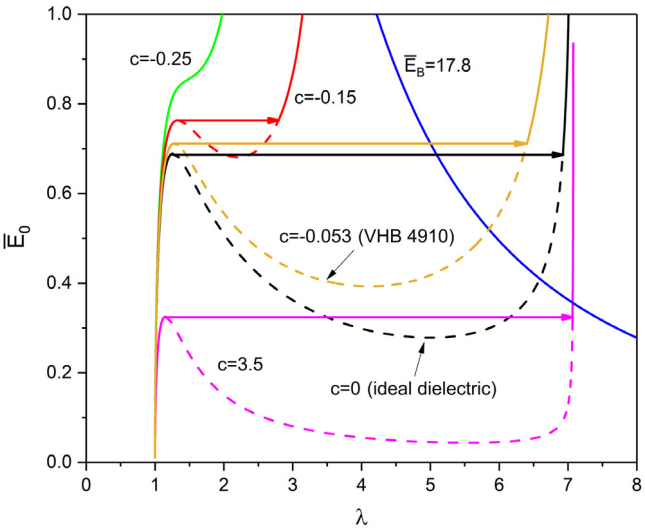

Fig. 14. Plots of $\overline{E}_0 \sim \lambda$ for a range of $c = -0.25, -0.15, -0.053, 0, 3.5$ for a DE plate with $G = 97.2$, $\overline{P} = 0$. We can see that electrostriction can significantly influence the critical values of both the onset and stop of snap-through instability.

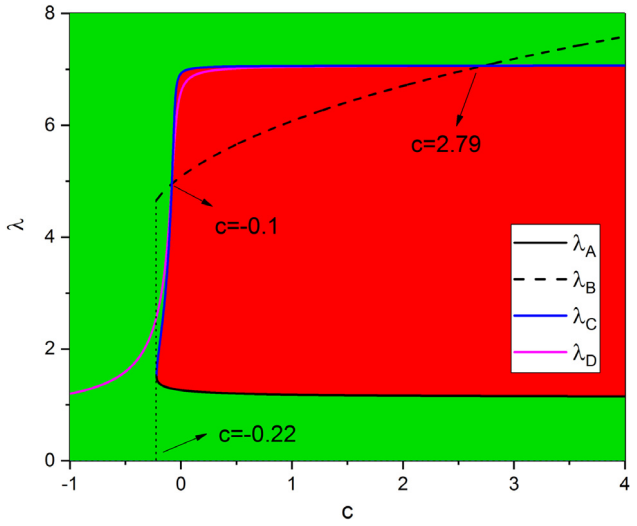

Fig. 15. Phase diagram of critical stretches of a DE plate with $G = 97.2$, $\overline{P} = 0$.

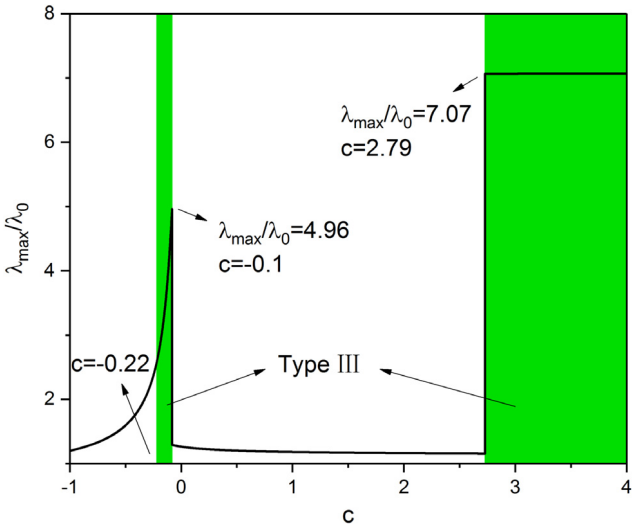

Fig. 16. Plot of λ_{max}/λ_0 versus c of a DE plate with $G = 97.2$, $\overline{P} = 0$.

are also examined in Figs. 13 and 15, respectively. For the case $c \geq -0.22$, as c decreases, $\overline{E}_A$ increases while $\overline{E}_C$ changes non-monotonically. Material with $c > 2.79$ is a type III DE and increasing of c will result in the decreasing of both $\overline{E}_A$ and $\overline{E}_C$, while with λ_A and λ_C almost remain unchanged. As c decreases, $\overline{E}_C$ increases first and then falls but with $\overline{E}_C$ always above $\overline{E}_B$, implying that the plate will fail by electrical breakdown during the snap-through process. With continuously decreasing of c, $\overline{E}_C$ decreases further and eventually the plate behaves like a type III DE again. It should be noted that the applied voltage needed to activate the snap-through instability for plate with $-0.22 < c < -0.1$ is much larger than that needed for plate with $c > 2.79$ (see Fig. 13) and that the acquired actuation stretch is much smaller (see Fig. 16). Thus the optimal c should lie in the region $c > 2.79$ and material with larger c performs better. It should be noted that for plate with $c > 2.79$, λ_D is always a little larger than λ_C, even though they are very close (Fig. 15), indicating that the plate may survive the snap-through instability at λ_C and can be stretched a little further to λ_D, where electrical breakdown happens (see the curve of $c =$ 3.5 in Fig. 14). The snap-through instability of a DE plate with $c < -0.22$ will be suppressed but a considerably large voltage is needed to reach the maximal allowable stretch λ_{max}. Nevertheless, the maximal allowable actuation stretch λ_{max}/λ_0 is really small, and this kind of DE is therefore not recommended.

Fig. 17 displays the influences of prestress $\overline{P}$ and material stretchability G on the $\log_{10}\overline{E} \sim c$ phase diagram of a DE plate. It can be seen that increasing $\overline{P}$ or decreasing G may decrease $\overline{E}_C$, and the plate subjected to a sufficiently large $\overline{P}$ or with a sufficiently small G will always survive the snap-through instability for any given c.

4. Conclusions

DEs show great potential for applications in smart devices. A critical issue related to their development is the prediction of instabilities that may occur in practical applications. Of particular attention is the so-called snap-through instability, with which giant actuation deformation can be gained. Based on the nonlinear electroelasticity and the Hessian method, the nonlinear response

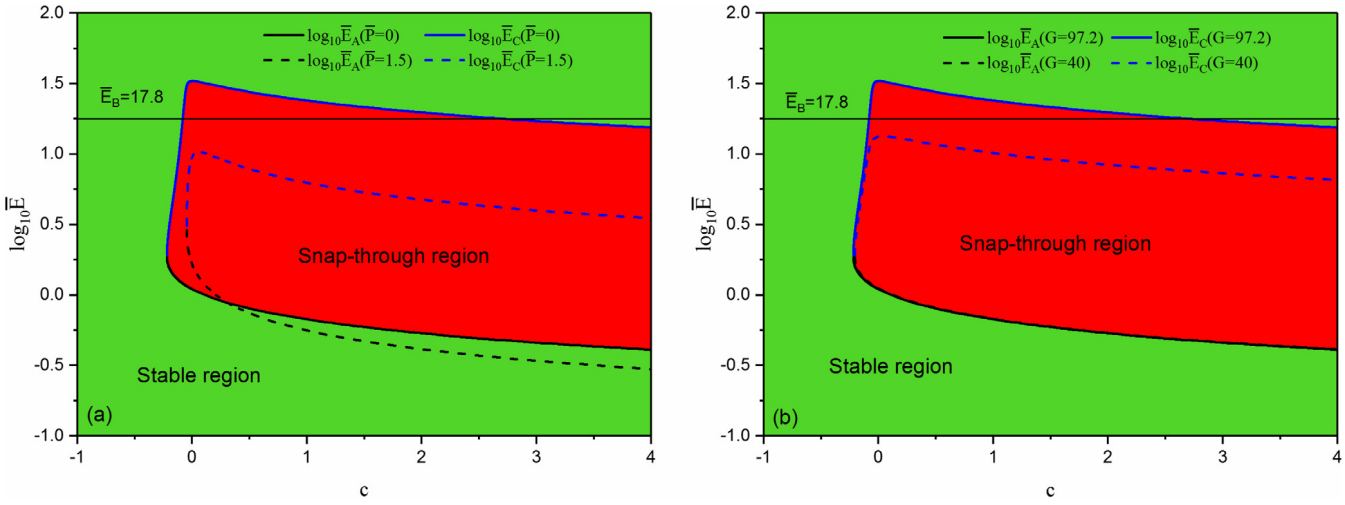

Fig. 17. Phase diagram $\log_{10}\bar{E} \sim c$ of a DE plate with (a) constant $G = 97.2$ and various $\bar{P}$; (b) constant $\bar{P} = 0$ and various G.

and snap-through stability of an incompressible Gent DE plate subjected to the combination of voltage and prestress are investigated. Results show that the plate deforms dramatically when the snap-through instability happens and this procedure can be effectively tuned by properly selecting the coefficient of electrostriction, ultimate material stretchability and prestress. Due to the strain-stiffening effect, Gent material will stop at a post-stable state after the snap-through instability happens, which is different from the neo-Hookean material. There exists a minimal coefficient of electrostriction (or maximal prestress), smaller (or larger) than which the snap-through instability may be suppressed. By calculating the threshold values of the onset and stop of snap-through instability of the plate, three kinds of phase diagrams are constructed, upon which a type III DE can be designed by properly tuning the electrostriction, material stretchability and/or prestress.

Most known dielectric elastomers belong to type I dielectric, i.e., with relatively small maximum actuation stretch (<100%, see Table 1 in Ref. [43]). It seems that a natural (i.e. without prestretching) type III dielectric elastomer with snap-through deformation completed prior to electrical breakdown has not been synthesized yet. Although experimental observations have suggested that applying prestress could improve the snap-through behavior of dielectric elastomers (see Fig. 12 in Huang et al. [44] who demonstrated that the prestressed circular disc of VHB 4905 could reach a giant voltage-induced strain before electric breakdown), the results in Figs. 10–12 of the current paper indicate that the actuation stretch induced by snap-through instability of a prestressed dielectric elastomer will be greatly reduced, or in other words, the snap-through behavior will be suppressed once a sufficiently large prestress is applied. Our calculations suggest from a theoretical standing point that tuning material constants (material stiffness and/or dielectricity) be the most effective way to achieve giant actuation stretch (or deformation in general). For example, we can design a type III dielectric material by choosing $G = 50.2$ or $c = 2.79$ to achieve a relatively large actuation stretch (>500%, see Figs. 7 and 16) without pre-stretching. Note that a bigger G or c does not mean a better performance. Thus, the material parameters should be optimized for a practical application. To the authors' best knowledge, this fact has never been noticed, and hence no experimental results could be found in the literature.

In summary, we studied in this work the effects of material stretchability and electrostriction on the snap-through instability of an incompressible Gent DE plate. The results indicated that material constants should be properly selected when designing a type III dielectric elastomer in its natural state (i.e. without pre-stretching). Such elastomers are very much desired in many practical applications where large electrically activated stretch or deformation is required. The present work provides a complete guidance to the design of natural type III dielectric elastomers.

Acknowledgments

This work was supported by the National Natural Science Foundation of China (Nos. 11532001, 11621062 and 11772295). It was also partly supported by the Fundamental Research Funds for the Central Universities (No. 2016XZZX001-05).

References

[1] P.G. de Gennes, Soft matter, Rev. Modern Phys. 64 (1992) 645–648.
[2] I.W. Hamley, Nanotechnology with soft materials, Angew. Chem. Int. Edn 42 (2003) 1692–1712.
[3] J. Kopeček, Hydrogel biomaterials: A smart future?, Biomaterials 28 (2007) 5185–5192.
[4] A. Goriely, M.G. Geers, G.A. Holzapfel, J. Jayamohan, A. Jérusalem, S. Sivaloganathan, W. Squier, J.A.W. van Dommelen, S. Waters, E. Kuhl, Mechanics of the brain: Perspectives, challenges, and opportunities, Biomech. Model. Mechan. 14 (2015) 931–965.
[5] R. Pelrine, R. Kornbluh, G. Kofod, High-strain actuator materials based on dielectric elastomers, Adv. Mater. 12 (2000) 1223–1225.
[6] A. O'Halloran, F. O'malley, P. McHugh, A review on dielectric elastomer actuators, technology, applications, and challenges, J. Appl. Phys. 104 (2008) 071101.
[7] F.B. Zhu, C.L. Zhang, J. Qian, W.Q. Chen, Mechanics of dielectric elastomers: materials, structures, and devices, J. Zhejiang Univ. Sci. A 17 (2016) 1–21.
[8] H.M. Wang, S.X. Qu, Constitutive models of artificial muscles: a review, J. Zhejiang Univ. Sci. A 17 (2016) 22–36.
[9] D. Chen, Q.B. Pei, Electronic muscles and skins: A review of soft sensors and actuators, Chem. Rev. 117 (2017) 11239–11268.
[10] K.H. Stark, C.G. Garton, Electric strength of irradiated polythene, Nature 176 (1955) 1225–1226.
[11] R. Díaz-Calleja, M.J. Sanchis, E. Riande, Effect of an electric field on the bifurcation of a biaxially stretched incompressible slab rubber, Eur. Phys. J. E 30 (2009) 417–426.
[12] A. Dorfmann, R.W. Ogden, Nonlinear electroelastostatics: Incremental equations and stability, Internat. J. Engrg. Sci. 48 (2010) 1–14.
[13] K. Bertoldi, M. Gei, Instabilities in multilayered soft dielectrics, J. Mech. Phys. Solids 59 (2011) 18–42.
[14] R. Diaz-Calleja, P. Llovera-Segovia, A. Quijano-López, Bifurcations in biaxially stretched highly non-linear materials under normal electric fields, Europhys. Lett. 108 (2014) 26002.
[15] J.Y. Zhou, L.Y. Jiang, R.E. Khayat, Electromechanical response and failure modes of a dielectric elastomer tube actuator with boundary constraints, Smart Mater. Struct. 23 (2014) 045028.
[16] W.M. Zhang, H. Yan, Z.K. Peng, G. Meng, Electrostatic pull-in instability in MEMS/NEMS: A review, Sensors Actuators A 214 (2014) 187–218.

[17] Y.P. Su, W.J. Zhou, W.Q. Chen, C.F. Lü, On buckling of a soft incompressible electroactive hollow cylinder, Int. J. Solids Struct. 97 (2016) 400–416.
[18] A. Goshkoderia, S. Rudykh, Electromechanical macroscopic instabilities in soft dielectric elastomer composites with periodic microstructures, Eur. J. Mech. A Solids 65 (2017) 243–256.
[19] J.S. Plante, S. Dubowsky, Large-scale failure modes of dielectric elastomer actuators, Int. J. Solids Struct. 43 (2006) 7727–7751.
[20] X.H. Zhao, Z.G. Suo, Method to analyze electromechanical stability of dielectric elastomers, Appl. Phys. Lett. 91 (2007) 061921.
[21] A.N. Norris, Comment on "Method to analyze electromechanical stability of dielectric elastomers [Appl. Phys. Lett. 91, 061921 (2007)]", Appl. Phys. Lett. 92 (2008) 026101.
[22] J.X. Zhou, W. Hong, X.H. Zhao, Z.Q. Zhang, Z.G. Suo, Propagation of instability in dielectric elastomers, Int. J. Solids Struct. 45 (2008) 3739–3750.
[23] J. Zhu, H. Stoyanov, G. Kofod, Z.G. Suo, Large deformation and electromechanical instability of a dielectric elastomer tube actuator, J. Appl. Phys. 108 (2010) 074113.
[24] S. Rudykh, K. Bhattacharya, Snap-through actuation of thick-wall electroactive balloons, Int. J. Non-Linear Mech. 47 (2012) 206–209.
[25] C. Keplinger, T.F. Li, R. Baumgartner, Z.G. Suo, S. Bauer, Harnessing snap-through instability in soft dielectrics to achieve giant voltage-triggered deformation, Soft Matter 8 (2012) 285–288.
[26] H.S. Park, Z.G. Suo, J.X. Zhou, P.A. Klein, A dynamic finite element method for inhomogeneous deformation and electromechanical instability of dielectric elastomer transducers, Int. J. Solids Struct. 49 (2012) 2187–2194.
[27] L.W. Liu, Y.J. Liu, X.J. Luo, B. Li, J.S. Leng, Electromechanical instability and snap-through instability of dielectric elastomers undergoing polarization saturation, Mech. Mater. 55 (2012) 60–72.
[28] L. An, F.F. Wang, S.B. Cheng, T.J. Lu, T.J. Wang, Experimental investigation of the electromechanical phase transition in a dielectric elastomer tube, Smart Mater. Struct. 24 (2015) 035006.
[29] S. Che, T.J. Lu, T.J. Wang, Electromechanical phase transition of a pressurized dielectric elastomer tube under mass control, Theor. Appl. Mech. Lett. 7 (2017) 121–125.
[30] T.F. Li, C. Keplinger, R. Baumgartner, S. Bauer, W. Yang, Z.G. Suo, Giant voltage-induced deformation in dielectric elastomers near the verge of snap-through instability, J. Mech. Phys. Solids 61 (2013) 611–628.
[31] H. Godaba, C.C. Foo, Z.Q. Zhang, B.C. Khoo, J. Zhu, Giant voltage-induced deformation of a dielectric elastomer under a constant pressure, Appl. Phys. Lett. 105 (2014) 112901.
[32] T.J. Lu, L. An, J. Li, C. Yuan, T.J. Wang, Electro-mechanical coupling bifurcation and bulging propagation in a cylindrical dielectric elastomer tube, J. Mech. Phys. Solids 85 (2015) 160–175.
[33] S.J.A. Koh, T.F. Li, J.X. Zhou, X.H. Zhao, W. Hong, W.J. Zhu, Z.G. Suo, Mechanisms of large actuation strain in dielectric elastomers, J. Polym. Sci. B 49 (2011) 504–515.
[34] A.N. Gent, A new constitutive relation for rubber, Rubber Chem. Technol. 69 (1996) 59–61.
[35] X.H. Zhao, Z.G. Suo, Electrostriction in elastic dielectrics undergoing large deformation, J. Appl. Phys. 104 (2008) 123530.
[36] M. Wissler, E. Mazza, Electromechanical coupling in dielectric elastomer actuators, Sensors Actuators A 138 (2007) 384–393.
[37] A. Dorfmann, R.W. Ogden, Nonlinear electroelastic deformations, J. Elasticity 82 (2006) 99–127.
[38] Z.G. Suo, X.H. Zhao, W.H. Greene, A nonlinear field theory of deformable dielectrics, J. Mech. Phys. Solids 56 (2008) 467–486.
[39] L. Dorfmann, R.W. Ogden, Instabilities of an electroelastic plate, Internat. J. Engrg. Sci. 77 (2014) 79–101.
[40] L. Dorfmann, R.W. Ogden, Nonlinear response of an electroelastic spherical shell, Internat. J. Engrg. Sci. 85 (2014) 163–174.
[41] L. Dorfmann, R.W. Ogden, Nonlinear electroelasticity: material properties, continuum theory and applications, Proc. R. Soc. Lond. Ser. A Math. Phys. Eng. Sci. 473 (2017) 20170311.
[42] R. Pelrine, R. Kornbluh, Q.B. Pei, J. Joseph, High-speed electrically actuated elastomers with strain greater than 100%, Science 287 (5454) (2000) 836–839.
[43] R. Pelrine, R. Kornbluh, J. Joseph, R. Heydt, Q.B. Pei, Q.S. Chiba, High-field deformation of elastomeric dielectrics for actuators, Mater. Sci. Eng. C 11 (2) (2000) 89–100.
[44] J.S. Huang, T.F. Li, C. Chiang Foo, J. Zhu, D.R. Clarke, Z.G. Suo, Giant voltage-actuated deformation of a dielectric elastomer under dead load, Appl. Phys. Lett. 100 (4) (2012) 041911.